Targeted Mutations in the *psaC* Gene of *Chlamydomonas reinhardtii*: Preferential Reduction of F_B at Low Temperature Is Not Accompanied by Altered Electron Flow from Photosystem I to Ferredoxin†

Nicolas Fischer,‡ Pierre Sétif,§ and Jean-David Rochaix*,‡

Departments of Molecular Biology and Plant Biology, University of Geneva, 30 quai Ernest-Ansermet, Switzerland, and CEA, Département de Biologie Cellulaire et Moléculaire, CNRS, URA 2096, C. E. Saclay, 91191, Gif-sur-Yvette Cedex, France

Received September 5, 1996; Revised Manuscript Received October 29, 1996⊗

ABSTRACT: The terminal part of the electron pathway within the photosystem I (PSI) complex includes two [4Fe-4S] centers, F_A and F_B, which are coordinated by the PsaC subunit. To gain new insights into the electron transfer mechanisms through PsaC, we have generated three mutant strains of the alga *Chlamydomonas reinhardtii* in which two positively charged residues, K_{52} and R_{53}, near the F_A center have been altered in different ways. The mutations $K_{52}S/R_{53}D$ and $K_{52}P/R_{53}D$ lead to a strong destabilization of PSI. The third mutant $K_{52}S/R_{53}A$ accumulates PSI to 30% of wild-type levels and shares the same residues between two of the cysteine ligands of F_A as the PsaC homologue in the green sulfur bacterium *Chlorobium limicola*, in which F_B has a higher redox potential than F_A [Nitschke, W., Feiler, U., & Rutherford, A. W. (1990) *Biochemistry 29*, 3834−3842]. Low-temperature electron paramagnetic resonance (EPR) studies reveal that, in contrast to wild type, F_B is preferentially photoreduced in this mutant, as was also observed for *C. limicola*. The preferential photoreduction of F_B could be due to changes in the redox potential of F_A and/or to slight structural modifications of the PsaC subunit. However, room temperature optical measurements show that stable charge separation still occurs and, surprisingly, that electron transfer from PSI to ferredoxin proceeds at normal rates in the mutant. As *C. limicola*, the $K_{52}S/R_{53}A$ and $K_{52}S/R_{53}D$ *C. reinhardtii* mutants are photosensitive when grown aerobically, but can grow photoautotrophically under anaerobic conditions.

Photosystem I (PSI)[1] is a multiprotein complex located in the thylakoid membranes of higher plants, algae, and cyanobacteria and acts as a light-driven plastocyanin−ferredoxin oxidoreductase. At least five chloroplast-encoded subunits (PsaA, -B, -C, -I, and -J) as well as six nuclear-encoded polypeptides (PsaD, -E, -F, -G, -H, and -K) form this complex (Golbeck, 1992). The redox components of the complex are bound by PsaA, PsaB, and PsaC. The large (80−85 kDa) PsaA and PsaB subunits bind the primary donor P700 (a chlorophyll dimer), the intermediate acceptors A_0 (a monomeric chlorophyll *a*), A_1 (a phylloquinone), and F_X (a [4Fe-4S] center) (Golbeck, 1992). The 8−9 kDa PsaC subunit is located on the stromal face of PSI and binds the two terminal [4Fe-4S] centers F_A and F_B (Hayashida et al., 1987; Høj et al., 1987; Oh-Oka et al., 1987). The two core subunits PsaA and PsaB can stably assemble *in vivo* in mutant strains of the cyanobacteria *Synechocystis* sp. PCC 6803 and *Anabaena variabilis* ATCC 29413 lacking PsaC (Yu et al., 1995; Mannan et al., 1991). In contrast, PsaC is required for stable accumulation of PSI in *Chlamydomonas reinhardtii* (Takahashi et al., 1991). The amino acid sequence of PsaC is highly conserved among species (Golbeck, 1992). It contains two CxxCxxCxxxCP motifs found in [4Fe-4S] center binding proteins. Cysteines 11, 14, 17, and 58 and cysteines 21, 48, 51, and 54 have been shown to coordinate the iron atoms of center F_B and F_A, respectively (Zhao et al., 1992). Sequence comparisons indicate that PsaC shares structural features with bacterial soluble ferredoxins containing two [4Fe-4S] clusters, and a model based on the structure of *Peptococcus aerogenes* ferredoxin has been proposed (Dunn & Gray, 1988; Figure 1). PsaC contains an additional internal loop probably interacting with the PSI core and a C-terminal extension which are absent in ferredoxins (Naver et al., 1996). The PSI crystal structure at 6 and 4.5 Å resolution clearly indicates the position of the [4Fe-4S] centers, one being closer to F_X and the other closer to the stromal surface (Krauss et al., 1993; Schubert et al., 1995). However, the identity of these centers has not yet been determined.

An important and unsolved question is the exact electron pathway between F_X and soluble ferredoxin. Some insights into the role of F_A and F_B have been gained through site-directed mutagenesis of their cysteine ligands. One approach has taken advantage of an *in vitro* reconstitution system in which a functional PSI complex is generated from the P700-F_X core and recombinant PsaC protein containing altered cysteine residues. (Zhao et al., 1992; Yu et al., 1993, 1995). Recently, *in vivo* mutagenesis of one cysteine ligand of F_B in *Anabaena variabilis* has shown that this center is not essential for electron transfer from PSI to ferredoxin (Mannan et al., 1996). Similar mutations in *C. reinhardtii* strongly

† This work was supported by a grant from the Human Frontier Science Program to P.S. and J.-D.R. and by Grant 31.34014.92 from the Swiss National Fund to J.-D.R.

* Corresponding author. Phone: 41 22 702 61 87. FAX: 41 22 702 68 68. Email: Rochaix@sc2a.unige.ch.

‡ University of Geneva.

§ CNRS.

⊗ Abstract published in *Advance ACS Abstracts,* December 15, 1996.

[1] Abbreviations: PSI, photosystem I; TAP, Tris−acetate−phosphate; HSM, high-salt medium (minimal medium); chl., chlorophyll; EPR, electron paramagnetic resonance; DPIP, 2,6-dichlorophenolindophenol.

S0006-2960(96)02244-1 CCC: $14.00

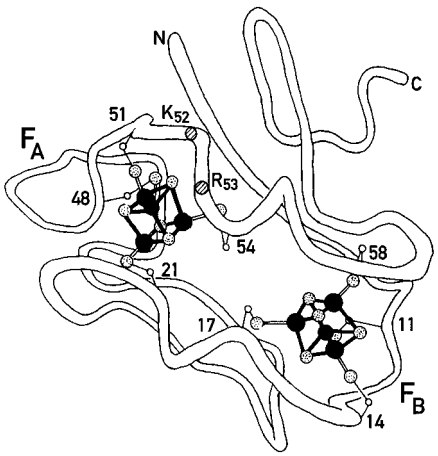

FIGURE 1: Model proposed for the structure of the PsaC subunit (Dunn & Gray, 1988). Cysteines which act as ligands for the two iron−sulfur centers F_A and F_B are numbered. Approximate positions of amino acids K_{52} and R_{53} are indicated.

destabilize the PSI complex (Takahashi et al., 1992). The observation that PsaC is required for accumulation of PsaA and PsaB in *C. reinhardtii* but not in *Synechocystis* sp. PCC6803 or in *A. variabilis* suggests that there are significant differences in the assembly and/or stabilization of the PSI complex in these organisms.

In most photosynthetic organisms, F_A has a higher redox potential than F_B, and F_A is preferentially photoreduced at 15 K. However, the situation is reversed in the green sulfur bacterium *Chlorobium limicola*. This organism contains a PSI-like complex with a PsaC homologue of 24 kDa that binds the two terminal [4Fe-4S] centers (Büttner et al., 1992). Center F_A has a lower redox potential than F_B which is the first center to be photoreduced at 15 K. In addition, both centers must have redox potentials at least 150 mV more negative than their PSI equivalents because they cannot be chemically reduced by sodium dithionite at high pH (Nitschke et al., 1990). Sequence comparison between PsaC and the 24 kDa protein of *C. limicola* shows that only 20% of the residues are conserved, mainly the cysteines involved in coordinating the [4Fe-4S] centers. The 24 kDa protein has a long positively charged N-terminal extension and many substitutions when compared to the PsaC sequence (Büttner et al., 1992). Among those differences, two positively charged amino acids of PsaC, Lys52 and Arg53, located between two cysteine ligands of F_A are replaced by serine and alanine in *C. limicola* (Figure 1). This observation raised the idea that these positively charged residues might be partly responsible for the less electronegative redox potential of F_A found in most photosynthetic organisms (Feiler & Hauska, 1995). To test this hypothesis, we have created several mutations which alter residues Lys52 and Arg53 in the PsaC subunit of *C. reinhardtii* and examined the electron transfer properties of PSI in these mutants.

MATERIALS AND METHODS

Strains and Media. *C. reinhardtii* wild-type and mutant strains were grown as described (Harris, 1989). If necessary, the media [Tris−acetate−phosphate medium (TAP) and high-salt minimal medium (HSM)] were solidified with 2% Bacto agar (Difco) and supplemented with spectinomycin (Sigma). For anaerobic liquid cultures, HSM medium was supplemented with 6 mM $Na_2S_2O_3$ and 4 μM Resazurin (an indicator of air exclusion) and bubbled with N_2 for 15 min. $NaHCO_3$ was added to a final concentration of 18 mM before inoculation. The Generbag anaer system (Biomérieux) was used for anaerobic growth conditions on plates.

Nucleic Acid Techniques. Procedures for the preparation of recombinant plasmids and DNA sequencing were performed as described (Sambrook et al., 1989). The bacterial host used was *E. coli* DH5α. *C. reinhardtii* total DNA was isolated as described previously (Rochaix et al., 1988). Southern blotting and hybridization were carried out as described (Southern, 1975; Sambrook et al., 1989). Site-directed mutations affecting K_{52} and R_{53} were introduced into the *psaC* gene using the following 36-mer oligonucleotide: 5′-GACTGTGTAGGTTGC(T/C)CAG(C/A)TTGTG AAA-CAGCTTGT-3′. Together with two other oligonucleotides complementary to the 5′ and 3′ ends of *psaC* carrying a *Nde*I and a *Bgl*II restriction site, respectively, we used the single tube polymerase chain reaction procedure described by Picard et al. (1994) to generate the mutant *psaC* genes. The amplified DNA fragments were gel-purified, digested with *Nde*I and *Bgl*II, and cloned into the plasmid pBSEP5.8 *aadA* [*Nde*I/*Bgl*II]. This plasmid contains a 5.8 *Eco*RI−*Pst*I fragment from the chloroplast *Eco*RI fragment R23 (Rochaix, 1978) with two unique *Nde*I and *Bgl*II restriction sites introduced at the 5′ and 3′ ends of the *psaC* coding sequence by a similar site-directed mutagenesis technique. This vector contains also an *aadA* expression cassette conferring spectinomycin and streptomycin resistance to *C. reinhardtii* (Goldschmidt-Clermont, 1991) inserted at a *Sal*I site 800 bp upstream of *psaC*.

Chloroplast Transformation. Chloroplast transformation in *C. reinhardtii* wild-type cells was carried out as described (Boynton et al., 1988) with a helium-driven particle gun adapted from the one designed by Finer et al. (1992). Wild-type cells were grown at 25 °C in liquid TAP media and plated on TAP plates supplemented with 150 μg/mL spectinomycin. Once the plates were dry, cells were bombarded with tungsten microprojectiles coated with the appropriate DNA. The bombarded cells were incubated for 2 weeks at 25 °C under low light (5 μE m^{-2} s^{-1}). Growing colonies were restreaked on fresh TAP plates containing 150 μg/mL spectinomycin and characterized.

Thylakoid Membranes and PSI Complex Purification. The procedure of Chua and Bennoun (1975) was slightly modified and carried out at 4 °C with minimal light exposure of the samples. Cells in exponential growth at 2×10^6 cells/mL were harvested by centrifugation at 2500*g*, washed in 0.3 M sucrose/25 mM Hepes−KOH (pH 7.5)/1 mM $MgCl_2$, and resuspended in the same buffer containing 1 mM PMSF at 2×10^8 cells/mL. Cells were broken in a chilled French press at 660 kg/cm^2 pressure. The homogenate was centrifugated at 2000*g* for 10 min and the pellet resuspended in 0.3 M sucrose/5 mM Hepes−KOH (pH 7.5)/10mM EDTA. The membranes were collected by centrifugation at 20000*g* for 10 min, and the pellet was resuspended in 1.8 M sucrose/5 mM Hepes−KOH (pH 7.5)/10 mM EDTA. This suspension was overlaid with an equal volume of 1.3 M sucrose/5 mM Hepes−KOH (pH 7.5)/10 mM EDTA and an equal volume of 0.5 M sucrose/5 mM Hepes−KOH (pH 7.5)/10 mM EDTA and centrifugated at 80000*g* for 1 h. The thylakoid membranes floating at the 1.3 and 0.5 M sucrose interfaces were collected, diluted with 3 volumes of 5 mM Hepes−KOH (pH 7.5)/10 mM EDTA, pelleted by centrifugation at

100000*g* for 1 h, and resuspended in 5 mM Hepes−KOH (pH 7.5)/10 mM EDTA for EPR measurements or in 400 mM sorbitol/15 mM NaCl/10 mM $MgCl_2$ for PSI complex purification.

To obtain PSI complex, the procedure of Takahashi et al. (1991) was slightly modified. Thylakoid membranes were pelleted by centrifugation at 20000*g*, washed with H_2O, pelleted at the same speed, and resuspended in H_2O at a chlorophyll concentration of 0.8 mg/mL; 10% (w/v) β-dodecyl maltoside (CalBiochem) was added to a final concentration of 0.9%, and the mixture was incubated for 20 min on ice. The solubilized thylakoids were centrifuged at 20000*g* for 10 min, and the supernatant was loaded on a 0.1−1 M sucrose density gradient containing 5 mM Tricine−NaOH (pH 8.0)/0.05% β-dodecyl maltoside. The gradients were centrifuged at 170000*g* for 16 h. The lower bands containing the PSI particles were collected and diluted with 3 volumes of 5 mM Tricine−NaOH, pH 8.0. The PSI particles were centrifuged at 250000*g* for 3 h, and the pellet was resuspended in the smallest possible volume. Note that this procedure does not include a NaBr wash of the thylakoids before solubilization. We noticed that this step often produced PSI complex with poor photochemical activity.

Western blot analysis was performed using the chemiluminescence detection system (Supersignal, Pierce). The amounts of protein detected were quantified using a Phosphoimager (Biorad) with a chemiluminescence screen.

Flash-Absorption and EPR Spectroscopies. Flash-induced absorption changes of P700/$P700^+$ were measured at 820 nm for both wild-type and $K_{52}S/R_{53}A$ PSI complexes. Subsaturating laser intensities were used in order to minimize changes due to the decay of antenna triplet states. For wild-type PSI, three main phases are observed with half-times of 10 μs (9%), 22 ms (46%), and 1.2 s (45 %). The major part of the fastest phase is probably due to decay of triplet states of antenna chlorophyll as its proportion decreases considerably at lower flash intensities. The slowest phase depends on the DPIP concentration and can be ascribed to reduction of $P700^+$ by reduced DPIP in reaction centers where electron escape from $[F_A\ F_B]^-$ to an exogenous acceptor (rate k_e) has occurred. The intermediate phase presumably corresponds to the recombination reaction between $P700^+$ and $[F_A\ F_B]^-$ (rate k_r). However, this recombination reaction competes with escape from $[F_A\ F_B]^-$ so that the observed rate corresponds to $k_r + k_e$. The ratio between the intermediate and the slowest phase corresponds to k_r/k_e, thus allowing us to derive the value of k_r ($\approx$15.9 s^{-1}). The absorption decay is more complicated in the case of PSI from the $K_{52}S/R_{53}A$ mutant, with the presence of four different phases (half-times of 20 μs, 1.6 ms, 27 ms, and 1.2 s with proportions of 14, 13, 37, and 36%, respectively). The two slowest components can be interpreted similarly to the equivalent components observed in wild-type PSI. Electron escape from $[F_A\ F_B]^-$ exhibits about the same rate as the recombination reaction ($k_r/k_e \approx 1$, as in wild-type PSI), and the recombination rate can be calculated ($\approx$13.0 s^{-1}). The two fastest phases are mostly due to intrinsic components of PSI photochemistry as their proportions decrease little at lower flash intensities. The 20 μs phase may correspond both to $^3P700$ decay formed from the primary radical pair $[P700^+\ A_0^-]$ and to a recombination reaction between $P700^+$ and A_1^-. The 1.6 ms phase may be due to a recombination reaction between $P700^+$ and F_X^-. Decay kinetics of $P700^+$ at 820 nm and ferredoxin reduction at 580 nm were recorded at 296 K with a microsecond time resolution as described previously (Sétif & Bottin, 1994, 1995). Low-temperature EPR spectroscopy was performed with a Bruker ESR300D X-band spectrometer equipped with an Oxford Instruments helium cryostat. Spin quantitations were performed as described in Lelong et al. (1994). For these measurements, EPR conditions (20 K, 2 mW of microwave power) were chosen in order to avoid microwave saturation of the signal due to iron−sulfur centers and radical signals which were eliminated before integration. The ratio $[F_B^-/F_A^-]$ was determined by estimating the relative areas of the absorption-like peaks in the low-field region (g_z peaks) under nonsaturating conditions for both the wild type and the mutant. This estimation can be performed when the other *g*-values of the species under consideration are known (Aasa & Vänngard, 1975).

RESULTS

Site-Directed Mutagenesis of the psaC Gene. We used an oligonucleotide with 2-fold degeneracy at the K_{52} and R_{53} codons, allowing the generation of DNA fragments carrying four different combinations of mutations (see Materials and Methods for details). Lys52 could be changed either to serine or to proline and Arg53 to aspartate or alanine. After polymerase chain reaction, the products were cloned into plasmid pBSEP5.8 *aadA* [*Nde*I/*Bgl*II]. This plasmid contains a 5.8 *Eco*RI−*Pst*I fragment from the chloroplast genomic fragment R23 (Rochaix, 1978) with two unique *Nde*I and *Bgl*II restriction sites introduced at the 5′ and 3′ ends of the *psaC* coding sequence. This vector also contains an *aadA* expression cassette conferring spectinomycin and streptomycin resistance to *C. reinhardtii* (Goldschmidt-Clermont, 1991) inserted at a SalI site 800 bp upstream of *psaC* (Takahashi et al., 1992). We first tested that transformants containing a wild-type *psaC* gene flanked by the new sites accumulate normal amounts of PsaC and have a phenotype identical to wild type under all conditions tested (data not shown). Three plasmids were obtained with the following combinations of mutations: $K_{52}S/R_{53}A$; $K_{52}S/R_{53}D$; $K_{52}P/R_{53}D$. These mutations also remove a Psp1406I restriction site that allows one to detect the mutation and to assess its degree of homoplasmicity in the transformants.

These constructs were introduced into wild-type *C. reinhardtii* cells via biolistic transformation (Boynton et al., 1988). Transformants were selected on TAP plates supplemented with 150 μg/mL spectinomycin and grown in dim light (5 μE m^{-2} s^{-1}). After recloning the transformants 3 times on the same media, Southern blot analysis was performed to confirm the presence of the mutations. Transformants containing homoplasmic genomes could be obtained for the three sets of mutations (Figure 2). The WT/80 lane shows that a single remaining wild-type genome copy could be detected under the hybridization conditions used.

Analysis of the Transformants. Measurements of fluorescence transients were performed on cells grown on TAP plates in dim light (5 μE m^{-2} s^{-1}) and dark-adapted for 15 min. Strains containing the $K_{52}S/R_{53}D$ and $K_{52}P/R_{53}D$ mutations displayed fluorescence transients characteristic of PSI-deficient strains (Chua et al., 1975; Bennoun et al., 1977). In contrast, the fluorescence transients of the $K_{52}S/R_{53}A$ mutant are very similar to wild type, suggesting that PSI is functional in this mutant (Figure 3).

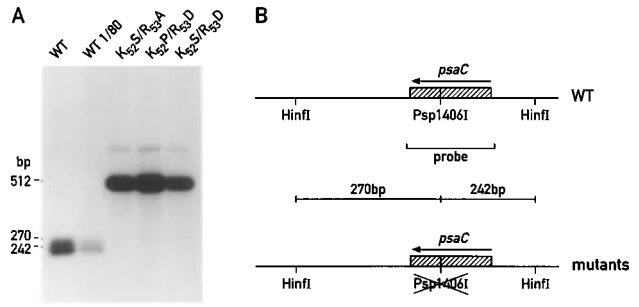

FIGURE 2: (A) Southern blot analysis performed on total genomic DNA from wild type and transformants carrying the mutations $K_{52}S/R_{53}A$, $K_{52}P/R_{53}D$, and $K_{52}S/R_{53}D$. The DNA was digested with *Hin*fI and Psp1406I restriction enzymes, separated by agarose gel electrophoresis, blotted, and hybridized with a ^{32}P-labeled radioactive probe spanning the *psaC* coding sequence. Lane WT/80 contains an 80-fold dilution of wild-type DNA to determine the sensitivity of detection. (B) Map of the chloroplast *psaC* region in wild-type and mutant strains. Restriction sites, expected fragments after digestion, and the probe used for Southern hybridization are indicated.

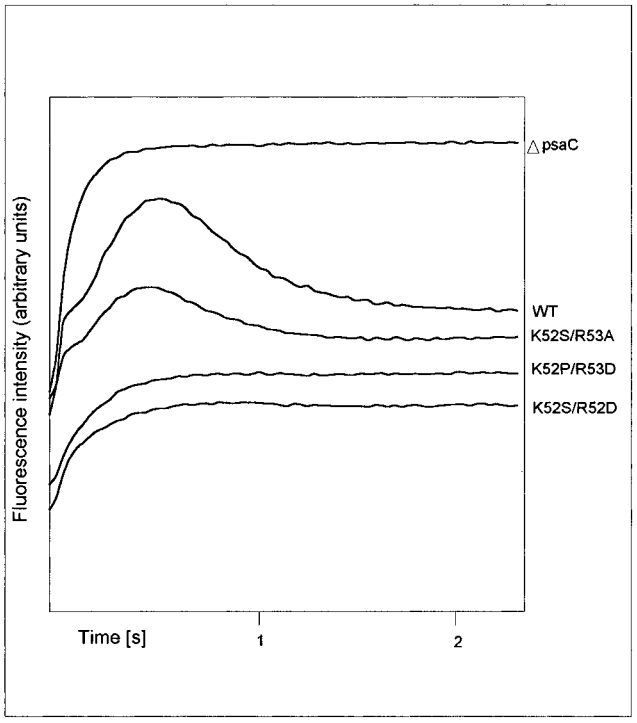

FIGURE 3: Fluorescence transients of dark-adapted cells of wild type, $K_{52}S/R_{53}A$, $K_{52}S/R_{53}A$, $K_{52}P/R_{53}D$, and of a strain lacking *psaC* (ΔpsaC). Cells were grown on TAP plates in low light (5 μE m^{-2} s^{-1}) and dark-adapted for 15 min before measurements.

Western blot analysis was performed on total cell extracts from liquid cultures grown in dim light to measure PSI accumulation. Figure 4 shows that mutants $K_{52}S/R_{53}D$ and $K_{52}P/R_{53}D$ accumulate very low amounts of PSI, similar to the level found in a strain in which *psaC* had been deleted (Fischer et al., 1996). This shows that these two sets of mutations destabilize the whole PSI complex. In the $K_{52}S/R_{53}A$ mutant, the PSI complex accumulated to 20−30% of wild-type levels. The signals obtained with D1 antibody show that PSII accumulation is not affected in these strains.

Growth phenotypes of the transformants and of the control strains grown on different media and under different light conditions are shown in Table 1. As expected, mutants $K_{52}S/R_{53}D$ and $K_{52}P/R_{53}D$ are unable to grow on minimal medium and are photosensitive. Mutant $K_{52}S/R_{53}A$ is also light-

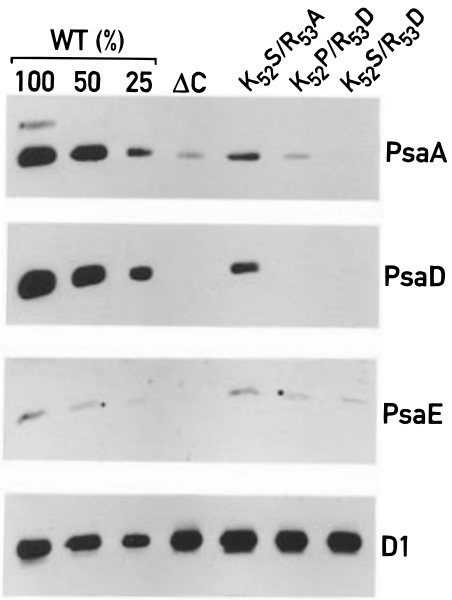

FIGURE 4: Western blot analysis of total cell extracts of wild type, $K_{52}S/R_{53}A$, $K_{52}P/R_{53}D$, $K_{52}S/R_{53}P$, and of a strain lacking *psaC*, grown in liquid TAP medium in low light (5 μE m^{-2} s^{-1}). 15 μg of total proteins was loaded per lane except for WT 50% and WT 25% where these relative amounts were loaded, respectively. Proteins were separated on a 15% SDS−PAGE, electroblotted on a nitrocellulose membrane, and probed with antibodies raised against subunits PsaA, PsaD, PsaE, and D1. The signals obtained were quantified as described under Materials and Methods. Panels are separated and do not correspond to the molecular weight of the proteins.

Table 1: Growth Properties of *psaC* Mutants[a]

	WT	ΔC	$K_{52}S/R_{53}A$	$K_{52}S/R_{53}D$	$K_{52}P/R_{53}D$
TAP_{DL}	+	+	+	+	+
TAP_{L}	+	−	slow	−	−
TAP_{HL}	+	−	−	−	−
HSM_{DL}	+	−	slow	−	−
HSM_{L}	+	−	−	−	−
HSM_{HL}	+	−	−	−	−
$TAP_{L,AN}$	+	−	+	slow	−
$HSM_{L,AN}$	+	−	+	slow	−

[a] DL = 5 μE m^{-2} s^{-1}; L = 60 μE m^{-2} s^{-1}; HL = 600 μE m^{-2} s^{-1}; AN = anaerobiosis; ΔC, mutant lacking *psaC*.

sensitive but is able to grow slowly on minimal medium in dim light (5 μE m^{-2} s^{-1}) or on TAP medium under a higher light intensity (60 μE m^{-2} s^{-1}). This phenotype cannot be explained by the lower PSI content because other mutant strains also affected in PSI accumulation (down to 10% of wild type levels) are able to grow on minimal medium at 60 μE m^{-2} s^{-1} light intensity (Kevin Redding and Mark Fleischmann, unpublished results).

Characterization of the PSI Complex from Wild Type and the $K_{52}S/R_{53}A$ Mutant. In order to examine and compare the biochemical and electron transfer properties of the PSI complex from $K_{52}S/R_{53}A$ mutant and wild-type cells, thylakoid membranes and PSI complex were purified from these two strains (see Materials and Methods). Previous work has shown that the PsaA, PsaB, and PsaD subunits are required for the stable integration of PsaC within the PSI complex (Li et al., 1991). Further, the PsaD and PsaE subunits do not assemble stably in PSI complex lacking PsaC (Yu et al., 1995). We first tested that the PSI complex isolated from the $K_{52}S/R_{53}A$ mutant had retained the subunits interacting with PsaC that could have been destabilized by the *psaC*

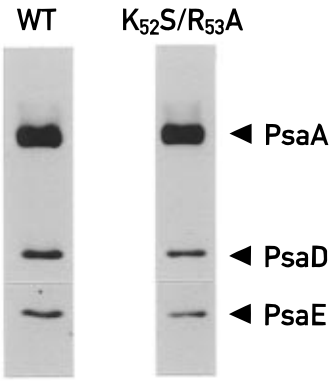

FIGURE 5: Western blot analysis of PSI complex purified from wild-type and $K_{52}S/R_{53}A$ strains. Proteins were separated as described in Figure 4 and probed with antibodies raised against subunits PsaA, PsaD, and PsaE on the same blot. Signals corresponding to PsaE were weaker and needed longer exposure. The signals were quantified as in Figure 4 to determine the amounts of PsaD and PsaE relative to the PsaA subunit.

mutations and therefore lost during purification of the complex. Western blot analysis of purified PSI complex from the mutant showed that it contained similar amounts of subunits PsaA, PsaD, and PsaE as compared to the wild-type complex (Figure 5).The intensities of the three bands were quantified (see Materials and Methods), and the amounts of PsaD and PsaE relative to the PsaA subunit were found to be over 90% identical between wild-type and mutant complexes. These mutations do therefore not appear to affect strongly the physical interactions between PsaC and PsaA, PsaD, or PsaE and the integrity of the PSI complex.

Measurements of flash-induced absorption changes at 820 nm revealed that 73% of the $K_{52}S/R_{53}A$ PSI complexes have retained all the redox cofactors of PSI and are able to perform a stable charge separation between $P700^+$ and $[F_A\ F_B]^-$ (data not shown, Table 2, see Materials and Methods for the measurement of the rate of recombination and escape from $[F_A\ F_B]^-$). These measurements also revealed that the mutant PSI is partially damaged with some complexes missing functional F_A and F_B (13%), thus undergoing a recombination reaction between $P700^+$ and F_X^-. Another portion of the mutant PSI complexes (14%) appears to be damaged at the level of the iron−sulfur center F_X or the phylloquinone A_1 which are either absent or not functional as electron acceptors (see Materials and Methods for details).

Light-Induced EPR Spectra at Low Temperature. It has long been recognized that PSI undergoes a stable charge separation between $P700^+$ and $[F_A\ F_B]^-$ at low temperature. This can be easily observed by EPR experiments performed below 30 K with samples poised with ascorbate and DPIP and preincubated at room temperature in darkness in order to reduce $P700^+$. Upon photoreduction at low temperature, F_A^- and F_B^- can be distinguished by their different EPR *g*-values ($g \approx 2.05$, 1.94, and 1.86 for F_A^-; $g \approx 2.07$, 1.92, and 1.89 for F_B^-). The upper part of Figure 6 shows the difference EPR spectrum (light minus dark) recorded at 15 K with wild-type PSI. A striking feature of this spectrum is the rather large amount of F_B^- (*g*-values of 2.070, 1.932, and 1.878) indicated by dotted lines on the KR spectrum, compared to F_A^- (*g*-values of 2.047, 1.945, and 1.857) marked by dotted lines on the WT spectrum ($[F_B^-/F_A^-] = 0.65 \pm 0.2$; see Materials and Methods for $[F_B^-/F_A^-]$ determination). In most other species, the EPR signals of F_B^- are considerably smaller than those of F_A^-. As a control, the same experiment was performed with wild-type thylakoids (lower part of Figure 6). Here too, the F_B^-/F_A^- ratio is rather large, though slightly smaller than in PSI. An unusual EPR signal is also observed around $g = 1.911$ in the difference spectrum (marked by * above dotted line). Due to the fact that it is also found in the thylakoid spectrum (*), this signal is probably not due to some damage of PSI but to an intrinsic feature of PSI in *C. reinhardtii* which is currrently under investigation [see also Hallahan et al. (1995)].

Similar experiments performed with the PSI complex from the $K_{52}S/R_{53}A$ mutant reveal that the F_B^- signal is largely dominating the spectrum ($[F_B^-/F_A^-] = 1.86 \pm 0.4$). Only the low-field peak of F_A^- is clearly observable (*g*-value of 2.049 in PSI and approximately 2.045 in thylakoids). The high-field peak of F_A^- is seen only as a shoulder on the broader high-field peak of F_B^- whereas the middle dispersion-like peak of F_A^- is probably obscured by the middle peak of F_B^-. The observed *g*-values for F_B^- differ only slightly from those observed in wild type (2.074, 1.931, and 1.875 in PSI and 2.073 in thylakoids).

It is important to know whether the preferential photoreduction of F_B in the mutant is accompanied by a change in the global efficiency of charge separation relative to the wild type. In the present study, this was tested by performing spin quantitations (see Materials and Methods) from the difference spectra obtained with wild-type and mutant PSI complexes which were carefully adjusted to the same concentrations of reaction centers with their full content of PSI redox components, determined by measuring the absorption transients at 820 nm (see above). This comparative analysis revealed that the efficiency of charge separation is similar in both types of PSI (Table 2). We conclude that significantly less F_A and more F_B are reduced in the mutant than in the the wild-type PSI complex.

EPR Spectra of Highly Reduced Samples. Samples were prepared in the presence of sodium dithionite at pH 10 and were illuminated before and after freezing in order to promote the (photo)reduction of all three PSI iron−sulfur centers F_A, F_B, and F_X. All three centers are observable at 15 K (part A of Figure 7) although the F_X^- signal is broadened at this temperature. It is well established that when both F_A and F_B centers are reduced, some new EPR signals emerge whereas some peaks ascribed to either F_A^- or F_B^- alone disappear. This is due to magnetic interactions between F_A^- and F_B^- which have been recently interpreted in a detailed model for the cyanobacterial PSI complex (Guigliarelli et al., 1993). In the latter, which is rather similar to PSI from higher plants (except for some broad side peaks), *g*-values at 2.050, 1.941, 1.916, and 1.885 are found for the coupled $[F_A^-\ F_B^-]$ spin system. The spectrum for $[F_A^-\ F_B^-]$ in *C. reinhardtii* reveals some novel features (Figure 7, part A, WT): *g*-values at 2.044, 1.962, 1.938, and 1.891 (indicated by dotted lines) are found with a shoulder around 2.06. The $[F_A^-\ F_B^-]$ spectrum of the mutant PSI complex differs slightly from its wild-type counterpart with *g*-values found at 2.051, 1.962, 1.941, 1.903, and 1.891 and a shoulder around 2.07. Spin quantitations were performed from both spectra and are shown in Table 2. Similar values are obtained for wild type and mutant, indicating that the content in iron−sulfur centers is comparable for both EPR samples. Part C of Figure 7 shows the g_x peak of F_X^- for both PSI

Table 2: Properties of Photosystem I from Wild-Type and the $K_{52}S/R_{53}A$ Mutant Strains of *C. reinhardtii*

	WT	KR
(a) General Properties		
chl *a*/chl *b*	3.8	4.0
recombination rate k_r (s^{-1}) between $P700^+$ and $[F_A, F_B]^-$ [a]	15.9, $t_{1/2} = 22$ ms	13.0, $t_{1/2} = 27$ ms
ratio between k_r and the rate of electron escape from $[F_A, F_B]^-$	1.0	1.0
subunit content (PsaA, PsaD, PsaE) (%)	100	90
amount of damaged PSI estimated from flash absorption studies (%)	<1	25
(b) Reduction of Ferredoxin from *Synechocystis* 6803 Measured at 580 nm		
second-order rate constant (M^{-1} s^{-1})	3.5×10^8	5.6×10^8
half-time of microsecond component (μs)	11.0 ± 1.5	11.5 ± 1.5
ratio between submicrosecond component and microsecond component	0.4 ($\pm$0.2)	0.3 ($\pm$0.15)
ferredoxin−PSI dissociation constant (μM)	6.1	7.3
(c) EPR Properties		
observed *g*-values for photoinduced signal at 15 K in PSI complexes	2.047/1.945/1.857 (F_A^-) 2.070/1.932/1.878 (F_B^-)	2.049 (F_A^-) 2.074/1.931/1.875 (F_B^-)
$[F_B^-/F_A^-]$	0.65 ± 0.2	1.86 ± 0.4
amount of spins for charge separation between $P700^+$ and $[F_A, F_B]^-$ [c]	10.0 ± 0.8	10.2 ± 0.8
observed *g*-values for fully reduced PSI complexes	$2.06^{(s)}$/2.044/1.962/1.938/1.891[d]	$2.07^{(s)}$/2.051/1.962/1.941/1.903/1.891
amount of spins for fully reduced samples	29.0 ± 5.0	31.4 ± 5.0
g_x-value of F_X^-	1.775	1.788
$^3P700$ signal: ratio of signal amplitudes found in presence of ascorbate and in fully reduced samples	0.04	0.19

[a] The recombination rate k_r was determined as explained under Materials and Methods. [b] See text. [c] See Materials and Methods for explanation. [d] Superscript (s), shoulder.

under conditions which are better suited for the observation of this center. Small differences are observed between the two types of PSI, with *g*-values of 1.775 and 1.788 for the wild type and the mutant, respectively.

Under such highly reducing conditions, it is believed that electron transfer is blocked at the level of the primary acceptor A_0^- due possibly to double reduction of the secondary acceptor, the phylloquinone A_1 (Sétif & Bottin, 1989). Charge separation between $P700^+$ and A_0^- is then followed by a recombination reaction which gives rise to the formation of the triplet state of P700, which is strongly polarized by the radical-pair mechanism (Hoff, 1981). The 2z peak of the $^3P700$ state is shown in part B of Figure 7 for both types of PSI. Wild-type and $K_{52}S/R_{53}A$ spectra were normalized in parts B, B′, and C of Figure 7 so that the intensities of the two triplet spectra observed in part B are identical. This procedure is used in order to display EPR signals corresponding to the same amount of core PSI containing at least the primary donor P700 and the primary acceptor A_0. Polarized P700 triplet was also recorded in samples prepared with ascorbate (part B′). For wild type, the triplet signal amounts to about 4% of the maximal signal observed (part B) whereas this proportion increases to a value of 19% in the mutant. These observations indicate that a small portion of F_X and/or A_1 has been damaged in the mutant PSI complex in agreement with the flash absorption studies at 820 nm.

Ferredoxin Reduction by PSI. Ferredoxin reduction has been previously studied in the cyanobacterium *Synechocystis* sp. PCC 6803 by measuring absorption changes in the 460−600 nm region (Sétif & Bottin, 1994, 1995). Due to the larger antenna size of PSI from *C. reinhardtii*, the present study of ferredoxin reduction is restricted to a single wavelength (580 nm). Figure 8 shows the absorption transients observed without (traces a) or with ferredoxin from *Synechocystis* sp. PCC 6803 (traces b, 2.02 μM; and c, 8.02 μM) for both types of PSI complexes. An absorption decrease due to electron transfer from the terminal [4Fe-4S] centers of PSI (F_A or F_B) to the [2Fe-2S] center of ferredoxin is observed in both cases (Sétif & Bottin, 1994, 1995). On a time scale of 6 ms (Figure 8, upper part), a concentration-dependent rate is observed. On a faster time scale of 400 μs, ferredoxin reduction can be observed after subtracting the absorption changes in the absence of ferredoxin from those in its presence (Figure 8, lower part). This subtraction procedure is made necessary by the presence of microsecond components ascribed to some triplet state antenna decay in the absence of ferredoxin. For both samples, a small unresolved component faster than 1 μs is observed as an immediate absorbance decrease with the present microsecond time resolution of the setup. This component is followed by a microsecond component with similar $t_{1/2}$ in both samples: 11.0 ± 1.5 μs and 11.5 ± 1.5 μs in the wild type and the mutant, respectively. The rate of this component is not dependent upon the ferredoxin concentration. It can therefore be ascribed to a first-order reduction of ferredoxin occurring in PSI/ferredoxin complexes which are performed before flash excitation (Sétif & Bottin, 1995). The amplitude of this microsecond component appears to increase with the ferredoxin concentration in parallel with the amplitude of the submicrosecond component. However, the magnitude of this last component is difficult to determine precisely owing to the poor signal to noise ratio of the present experiments. The ratios between the magnitude of the submicrosecond component and that of the microsecond component are about 0.4 ($\pm$0.2) and 0.3 ($\pm$0.15) in the wild type and the mutant, respectively. The sum of the magnitudes of these components is plotted as a function of ferredoxin concentration in the upper part of Figure 9. These data were fitted assuming a simple binding equilibrium

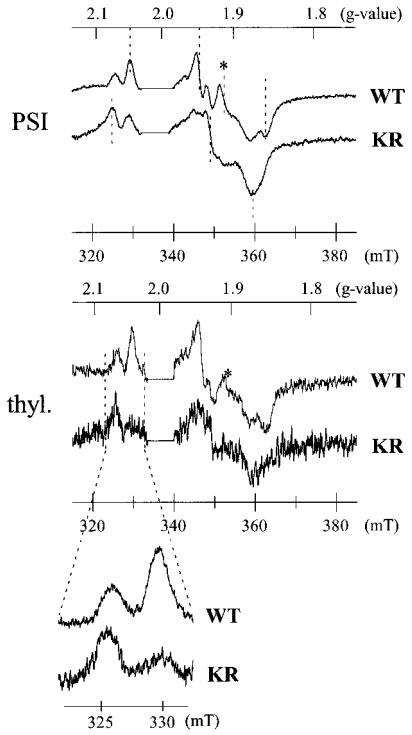

FIGURE 6: Light-induced EPR spectra of PSI complexes (upper part) and thylakoid membranes (middle and lower parts) from wild-type (WT) and $K_{52}S/R_{53}A$ (KR) strains from *C. reinhardtii*. Each of these spectra corresponds to the difference between spectra recorded after a 2 min illumination at 15 K and in darkness. The region around 335 mT ($g \approx 2.0$) exhibits a large radical signal due to $P700^+$ and is not shown. EPR conditions: temperature, 15 K; microwave power, 20 mW; modulation amplitude, 1 mT; microwave frequency, 9.435 GHz for PSI and 9.406 GHz for thylakoids; sum of 8 scans (uppper part), 2 scans (middle part), or 16 scans (lower part). Upper part: dotted lines indicate peaks ascribed to F_A^- and F_B^- on the wild-type and KR spectrum, respectively. The EPR tubes containing PSI complexes were prepared with identical concentrations of stable $P700^+$ (5.0 μM) as determined by flash-absorption spectroscopy at 820 nm. This corresponds to 0.84 mg of chl/mL and 1.42 mg of chl/mL for the wild type and the mutated PSI, respectively. The chlorophyll concentration of EPR tubes containing thylakoids is about 2.5 mg of chl/mL. In this case, the mutant spectra were multiplied by a factor of 2 in order to normalize the intensities of the F_X^- signals that were recorded on the same tubes under highly reducing conditions. All samples were prepared in Tricine, 20 mM, pH 8, in the presence of 5 mM sodium ascorbate and 50 μM DPIP. Tubes were incubated at room temperature for 2 min in darkness before freezing in darkness.

between PSI and ferredoxin, thus providing dissociation constants of 6.1 μM and 7.3 μM for the wild type and the mutant, respectively. The lower part of Figure 9 displays the dependence of the rate of the slow component on the ferredoxin concentration. The linear relationship found in both wild-type and mutant shows that this component is due to a second-order process of ferredoxin reduction by PSI. Linear fits provide second-order rate constants of 3.5×10^8 M^{-1} s^{-1} and 5.6×10^8 M^{-1} s^{-1} for the wild type and the mutant, respectively. These experiments show that the mutant PSI complex transfers electrons to ferredoxin at rates very similar to wild type and that the affinity of ferredoxin for this complex is not altered. Properties of wild type and $K_{52}S/R_{53}A$ PSI complexes that are described above are summarized in Table 2.

Oxygen Sensitivity of the Mutant Strains. The observation that $K_{52}S/R_{53}A$ PSI is able to perform charge separation and to transfer electrons to ferredoxin *in vitro* and that it

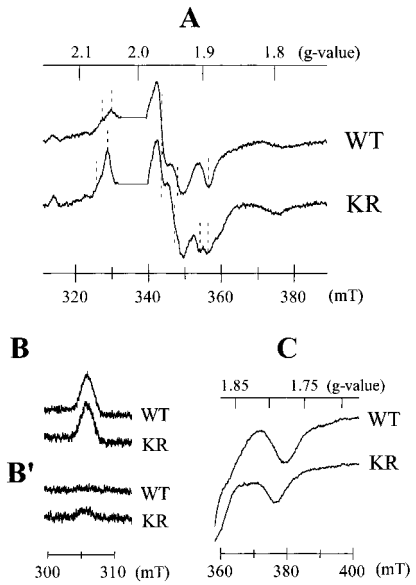

FIGURE 7: EPR spectra of PSI complexes from wild-type (WT) and $K_{52}S/R_{53}A$ (KR) strains prepared under highly reducing conditions (parts A, B, and C) or under conditions identical to those of Figure 6 (ascorbate/DPIP, part B′). In parts A, B, and C, both samples were prepared in the presence of 20 mM sodium dithionite at pH 10 (glycine−NaOH, 100 mM) and were illuminated for 1 min at room temperature before freezing under illumination. Spectra of parts A and C were recorded in darkness whereas spectra of parts B and B′ were recorded under strong illumination. Part A: temperature, 15 K; microwave power, 2 mW; modulation amplitude, 1 mT. Dotted lines indicate peaks except for the first lines on the left of the spectrum which indicate shoulders (see text). Parts B and B′: 2*z* peak of the $^3P700$ state; temperature, 4.2 K; microwave power, 0.2 mW; modulation amplitude, 2 mT. Part C: g_x peak of F_X^-; temperature, 9 K; microwave power, 80 mW; modulation amplitude, 1 mT. Microwave frequency: 9.437 for WT and 9.436 for KR. As in Figure 6, PSI complexes were prepared with identical concentrations of stable $P700^+$ (5.0 μM) as determined by flash-absorption spectroscopy at 820 nm. For parts B, B′, and C, the KR spectra were multiplied by a factor of 0.77. This factor was chosen in order to normalize the intensities of the $^3P700$ spectra observed under highly reducing conditions (part B).

accumulates *in vivo* at levels sufficient to ensure photoautotrophic growth was clearly in disagreement with the growth phenotype of the $K_{52}S/R_{53}A$ mutant strain (Table 1). It is known that [4Fe-4S] centers are very sensitive to oxidizing substances (Petering et al., 1971; Hardy & Burns, 1973) and that centers oxidized beyond their normal oxidation state are irreversibly damaged (Stiefel & George, 1994). To test whether oxygen could be responsible for the mutant growth phenotype, we grew mutant and control strains in minimal and TAP media under anaerobic conditions in the presence of light. The results presented in Table 1 clearly show that under anaerobiosis the $K_{52}S/R_{53}A$ mutant strain is able to grow at normal rates on minimal and TAP media at a light intensity of 60 μE m^{-2} s^{-1}. Furthermore, the $K_{52}S/R_{53}D$ mutant strain is capable of slow growth on minimal and TAP media under the same conditions, suggesting that a least some functional PSI is assembled in this mutant under anaerobiosis.

DISCUSSION

Preferential Photoreduction of F_B at Low Temperature in the PsaC $K_{52}S/R_{53}A$ Mutant. Earlier attempts to study the electron transfer properties of *C. reinhardtii* mutants with altered cysteine ligands of the [4Fe-4S] centers F_A and F_B were unsuccessful because these mutants failed to accumulate

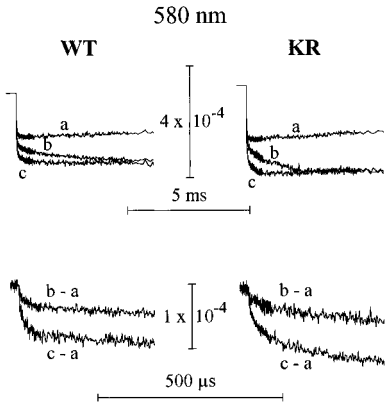

FIGURE 8: Flash-induced absorption changes measured at 580 nm with PSI complexes from *C. reinhardtii* with or without ferredoxin from *Synechocystis* 6803. Samples were prepared from the wild-type (WT; left part) and the $K_{52}S/R_{53}A$ (KR; right part) strains. The PSI complexes were suspended in 20 mM Tricine, pH 8, in the presence of 0.03% β-DM, 30 mM NaCl, 5 mM $MgCl_2$, 1 mM sodium ascorbate, and 8 μM DPIP. The absorbances of the samples were 1.33 at 678.9 nm and 2.92 at 679.7 nm for the wild type and the mutant, respectively. The corresponding concentrations of slowly recombining $P700^+$ concentrations (measured at 820 nm and corresponding to electron transfer to $[F_A\ F_B]$) are respectively 0.130 μM and 0.169 μM for the wild type and the mutant. Traces a are observed in the absence of ferredoxin whereas traces b and c were observed in the presence of 2.02 and 8.02 μM ferredoxin, respectively. In the lower part, ferredoxin reduction is displayed on a faster time scale by subtracting curves a from curves b and c. Traces are averages of 64 (WT) or 128 (KR) experiments. A delay of 10 s was used between two consecutive flashes.

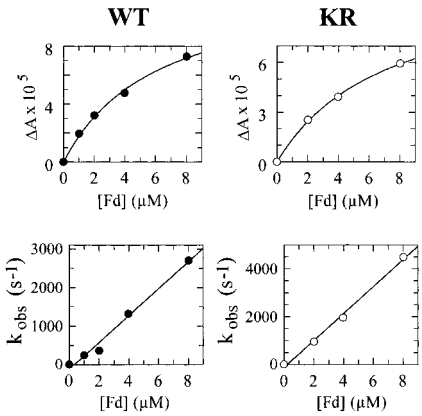

FIGURE 9: Kinetic characteristics of the ferredoxin reduction process for both the wild-type (WT; left part) and the $K_{52}S/R_{53}A$ (KR; right part) strains. Absorption changes similar to those shown in Figure 8 were used for computing these kinetic parameters (same samples studied under similar conditions). The upper part shows the signal amplitude measured at 60 μs after the flash on traces exhibiting directly ferredoxin reduction (see traces b−a and c−a in Figure 8). These amplitudes are negative, and absolute values are shown here. Assuming that these signals correspond to bound ferredoxin (see text), the two curves were fitted considering a simple binding equilibrium between free and bound ferredoxin. For fitting the data, the PSI concentrations were assumed to have constant values corresponding to slowly recombining $P700^+$ (0.130 μM and 0.169 μM for WT and KR, respectively). The dissociation constants, K_d, were estimated at 6.1 μM and 7.3 μM for the WT and the mutant, respectively. The lower part shows the dependence of the rate of the slower phase of ferredoxin reduction on the concentration of ferredoxin. A linear fit of the data is shown. It corresponds to k_{obs} $(s^{-1}) = [Fd] \times (3.5 \times 10^8\ M^{-1}\ s^{-1})$ for the wild type and to $k_{obs} = [Fd] \times (5.6 \times 10^8\ M^{-1}\ s^{-1})$ for the mutant.

significant amounts of PSI (Takahashi et al., 1992). Here we have taken an alternative approach aimed at creating milder changes affecting electron transfer within PsaC without destabilizing the entire PSI complex. We modified charged residues located in close proximity of the [4Fe-4S] center F_A in the PsaC subunit of *C. reinhardtii.* Residues K_{52} and R_{53} were selected for two reasons. First, they are located between C_{51} and C_{54} that act as ligands for center F_A (Zhao et al., 1992). Second, in *C. limicola*, which possesses a PSI-like complex with a PsaC-related subunit containing similar [4Fe-4S] centers, serine and alanine residues are found in these positions. In this organism, the redox potentials of F_B and F_A are inverted relative to oxygenic photosynthetic organisms. Hence, in *C. limicola* F_B is preferentially reduced at low temperature instead of F_A as in most photosynthetic organisms examined (Nitschke et al., 1990). These observations raised the possibility that residues K_{52} and R_{53} could play some role in setting the redox potential of F_A to a less negative value.

The $K_{52}S/R_{53}A$ mutant strain accumulates 20−30% PSI and displays fluorescence transients similar to wild type. The most striking result revealed by EPR is that F_B is preferentially photoreduced at 15 K in the mutant as found in *C. limicola.* While we cannot exclude that structural changes within PsaC are responsible for this phenotype, the data suggest that the redox potential of F_A is more negative in the mutant than in the wild type. Although it is not clear if the relative populations of the states $[F_A^-\ F_B]$ and $[F_A\ F_B^-]$ observed at cryogenic temperatures represent the equilibrium between the two states at room temperature (K. Brettel, personal communication), it is likely that this equilibrium is also modified in the mutant at room temperature.

Optical Spectroscopic Analysis of the $K_{52}S/R_{53}A$ Mutant. Spectroscopic analysis at 820 nm of the PSI complex from the $K_{52}S/R_{53}A$ mutant revealed that it is functional as measured by its ability to perform stable charge separation between $P700^+$ and $[F_A\ F_B]^-$. However, this analysis also revealed that the PSI complex from the mutant is more fragile since close to 25% of this complex had damaged redox cofactors.

The present study has allowed us to determine the kinetics of ferredoxin reduction by PSI in *C. reinhardtii* by measuring the time course of absorption changes at 580 nm. This transient comprises a fast phase with a half-time of 11 μs corresponding to a first-order reduction of ferredoxin within a PSI−ferredoxin complex. The dissociation constant of this complex is around 6 μM, which is circa 10-fold larger than the corresponding value determined for complex formation between ferredoxin from *Synechocystis* sp. PCC 6803 and PSI from either spinach or *Synechocystis* sp. PCC 6803 (Sétif & Bottin, 1995). A dissociation constant of 6 μM was also found with both wild-type PSI and ferredoxin isolated from *C. reinhardtii* (N. Fischer, P. Sétif, and J.-D. Rochaix, unpublished results). This suggests that the decrease in affinity of ferredoxin in *C. reinhardtii* is due to some property of PSI from *C. reinhardtii* which appears to be different in this respect from PSI of spinach and *Synechocystis.* The slower kinetic compound reflects a second-order process of ferredoxin reduction by PSI with a second-order rate constant of $3.5 \times 10^8\ M^{-1}\ s^{-1}$ for the wild type which is similar in the mutant. Hence, surprisingly, in spite of the preferential photoreduction of F_B at low temperature in the $K_{52}S/R_{53}A$ PSI complex, the transfer of electrons to ferredoxin occurs with rates and kinetics comparable to the wild-type complex. The fact that no significant difference between mutant and wild type could be observed for the fast components of

electron transfer to ferredoxin suggests that there is a rapid electron exchange between the two centers F_A and F_B which is not limiting for forward electron transfer. Yu et al. (1995) reported that a [4Fe-4S] center (named F_A') liganded by three cysteines and an aspartate in position 51 had a largely modified redox potential of −630 mV but was functional at room temperature and $NADP^+$ reduction mediated by both ferredoxin and flavodoxin was unchanged in this mutant complex. The authors explained these results by the overall large Gibbs free energy change between F_X and ferredoxin, acting as a driving force against the modified redox potential. Recently, a $C_{13}D$ PsaC mutant of *A. variabilis* lacking F_B was also shown to sustain normal rates of $NADP^+$ reduction (Mannan et al., 1996). The possibility that ferredoxin reduction by PSI might not be the rate-limiting step in $NADP^+$ reduction could explain these results. It is noteworthy that low-temperature EPR reveals that the F_A^-/F_B^- ratio determined for wild-type PSI from *C. reinhardtii* is significantly lower than the value obtained for other oxygenic photosynthetic organisms with the exception of barley and *P. laminosum* (Nugent et al., 1981; Cammack et al., 1979).

Ferredoxin and flavodoxin binding sites on PSI have been determined on cross-linked PSI−ferredoxin complexes (Lelong et al., 1996; Mülenhoff et al., 1996) in agreement with the binding site predicted by modeling (Fromme et al., 1994). Both sites are located next to the outermost center, suggesting that it is the electron-donating center. If one accepts that the new equilibrium distribution between $[F_A^-\ F_B]$ and $[F_A\ F_B^-]$ in the mutant at low temperature is mainly due to the altered redox potential of F_A and given the unchanged fast kinetic component of ferredoxin reduction, all of these data would best fit if the electron-donating center is F_B. Clearly, this interpretation remains speculative. However, targeted mutagenesis of charged amino acids in close proximity of the [4Fe-4S] centers appears to be a promising approach for analyzing electron transfer within PsaC, in particular in the eukaryotic alga *C. reinhardtii* where mutagenesis of cysteines involved in liganding F_A and F_B leads to the instability of the PSI complex.

Photosensitivity of the Mutant PSI Complex Is Diminished under Anaerobic Conditions. In this study, we have generated three different psaC double mutants containing the mutations $K_{52}S/R_{53}A$, $K_{52}S/R_{53}D$, and $K_{52}P/R_{53}D$. The last two mutants are unable to accumulate PSI under normal conditions. However, a striking feature of the $K_{52}S/R_{53}A$ and $K_{52}S/R_{53}D$ mutant strains is their light sensitivity under aerobic conditions and their ability to grow on minimal medium under anaerobic conditions. It is known that [4Fe-4S] centers are denatured by oxidizing substances, as described for different proteins such as hydrogenase and nitrogenase (Hardy & Burns, 1973). Superoxide has recently been shown to be responsible for the inactivation of several [4Fe-4S]-containing enzymes including aconitase, fumarase, and dihydroxy-acid dehydratase (Gardner & Fridovich, 1991; Flint et al., 1993). Solvent accessibility to the center is also an important parameter for its stability. Replacement of Tyr19 in the high-potential iron protein of *C. vinosum* by polar residues resulted in significant center instability (Agarwal et al., 1995). Although K_{52} and R_{53} are not hydrophobic residues, it is possible that structural modifications in the $K_{52}S/R_{53}A$ and $K_{52}S/R_{53}D$ PSI complexes alter solvent accessibility to the center and cause its degradation under aerobic conditions. Another possibility is that the modified redox potential of F_A could allow higher rates of electron escape to exogenous acceptors, generating oxidizing substances under continuous illumination and high electron flux through PSI. Oxygen sensitivity may also account for the partial instability of the $K_{52}S/R_{53}A$ PSI complex. In the $K_{52}S/R_{53}D$ mutant, the negative charge should modify the redox potential even more, leading to a more severe phenotype as observed in this study. In this context, it is also interesting to note that *C. limicola* grows exclusively under anaerobic conditions.

ACKNOWLEDGMENT

We thank K. Redding for providing antibodies raised against PsaA from *C. reinhardtii*, N. Roggli for preparing the figures, and K. Redding and M. Hippler for helpful comments.

REFERENCES

Aasa, R., & Vänngard, T. (1975) *J. Magn. Reson. 19*, 308−315.
Agarwal, A., Li, D., & Cowan, J. A. (1995) *Proc. Natl. Acad. Sci. U.S.A. 92*, 9440−9444.
Bennoun, P., Girard, J., & Chua, N.-H. (1977) *Mol. Gen. Genet. 153*, 343−348.
Boynton, J. E., Gilham, N. W., & Harris, E. H. (1988) *Science 240*, 1534−1538.
Büttner, M., Xie, D.-L., Nelson, H., Pinther, W., Hauska, G., & Nelson, N. (1992) *Proc. Natl. Acad. Sci. U.S.A. 89*, 8135−8139.
Cammack, R., Ryan, M. D., & Stewart, A. (1979) *FEBS Lett. 107*, 422−426.
Chua, N.-H., & Bennoun, P. (1975) *Proc. Natl. Acad. Sci. U.S.A. 72*, 2175−2179.
Chua, N.-H., Matlin, K., & Bennoun, P. (1975) *J. Cell Biol. 67*, 361−377.
Dunn, P. P. J., & Gray, J. C. (1988) *Plant Mol. Biol. 11*, 311−319.
Feiler, U., & Hauska, G. (1995) in *Anoxygenic photosynthetic bacteria* (Blankenship, R. E., Ed.) pp 665−685, Kluwer Academic Publisher, The Netherlands.
Finer, J. J., Vain, P., Jones, M. W., & McMullen, M. D. (1992) *Plant Cell Rep. 11*, 323−328.
Fischer, N., Stampacchia, O., Redding, K., & Rochaix, J.-D. (1996) *Mol. Gen. Genet. 251*, 373−380.
Flint, D. H., Tuminello, J. F., & Emptage, M. H. (1993) *J. Biol. Chem. 268*, 22369−22376.
Fromme, P., Schubert, W.-D., & Krauss, N. (1994) *Biochim. Biophys. Acta 1187*, 99−105.
Gardner, P. R., & Fridovich, I. (1991) *J. Biol. Chem. 266*, 19328−19333.
Golbeck, J. H. (1992) *Annu. Rev. Plant Physiol. Plant Mol. Biol. 43*, 293−324.
Goldschmidt-Clermont, M. (1991) *Nucleic Acids Res. 19*, 4083−4089.
Guigliarelli, B., Guillaussier, J., More, C., Sétif, P., Bottin, H., & Bertrand, P. (1993) *J. Biol. Chem.* 268, 900−908.
Hallahan, B. J., Purton, S., Ivison, A., Wright, D., & Ewans, M. C. W. (1995) *Photosynth. Res. 46*, 257−264.
Hardy, R. W. F., & Burns, R. C. (1973) in *Iron-Sulfur Proteins I* (Lovenberg, W., Ed.) pp 65−110, Academic Press, New York.
Hayashida, N., Matsubayashi, K., Shinozaki, M., Inoue, K., & Hiyama, T. (1987) *Curr. Genet. 12*, 247−250.
Hoff, A. J. (1981) *Q. Rev. Biophys. 17*, 153−282.
Høj, P. B., Swendsen, I., Scheller, H. V., & Møller, B. L. (1987) *J. Biol. Chem. 262*, 12676−12684.
Krauss, N., Hinrichs, W., Witt, I., Fromme, P., Pritzkow, W., Dauter, Z., Betzel, C., Wilson, K. S., Witt, H., & SWaenger, W. (1993) *Nature 361*, 326−331.
Lelong, C., Sétif, P., Lagoutte, B., & Bottin, H. (1994) *J. Biol. Chem. 269*, 10034−10039.
Lelong, C., Boekema, J., Kruip, J., Bottin, H., Rögner, M., & Sétif, P. (1996) *EMBO J. 15*, 2160−2168.

Li, N., Warren, P. V., Warden, J. T., Bryant, D. A., & Golbeck, J. H. (1991) *Biochemistry 30*, 7863−7872.

Mannan, M. R., Whitmarsh, J., Nyman, P., & Pakrasi, H. B. (1991) *Proc. Natl. Acad. Sci. U.S.A. 88*, 10168−10172.

Mannan, M. R., He, W.-Z., Metzger, S., Withmarsh, J., Malkin, R., & Pakrasi, H. B. (1996) *EMBO J. 15*, 1826−1833.

Mühlenhoff, U., Kruip, J., Bryant, D. A., Sétif, P., & Boekema, E. (1996) *EMBO J. 15*, 488−497.

Naver, H., Scott, M. P., Golbeck, J. H., Moller, B. L., & Scheller, H. V. (1996) *J. Biol. Chem. 271*, 8996−9001.

Nitschke, W., Feiler, U., & Rutherford, A. W. (1990) *Biochemistry 29*, 3834−3842.

Nugent, J. H. A., Møller, B. L., & Evans, M. C. V. (1981) *Biochim. Biophys. Acta 634*, 249−255.

Oh-Oka, H., Takahashi, Y., Wada, K., Matsubara, H., Ohyama, K., & Ozeki, H. (1987) *FEBS Lett. 218*, 52−54.

Petering, D., Fee, J. A., & Palmer, G. (1971) *J. Biol. Chem. 246*, 643−653.

Picard, V., Ersdal-Badju, E., Lu, A., & Bock, S. C. (1994) *Nucleic Acids Res. 22*, 2587−2591.

Rochaix, J.-D. (1978) *J. Mol. Biol. 126*, 597−617.

Rochaix, J.-D., Mayfield, S., Goldschmidt-Clermont, M., & Erickson, J. (1988) in *Plant Molecular Biology a practical approach* (Shaw, C. H., Ed.) pp 253−275, IRL Press, Oxford.

Schubert, W. D., Klukas, O., Krauss, N., Saenger, W., Fromme, P., & Witt, H. T. (1995) in *Photosynthesis: from light to Biosphere Vol. II* (Mathis, P., Ed.) pp 3−10, Kluwer Academic Publishers, Dordrecht, The Netherlands.

Sétif, P., & Bottin, H. (1989) *Biochemistry 28*, 2689−2697.

Sétif, P., & Bottin, H. (1994) *Biochemistry 33*, 8495−8504.

Sétif, P., & Bottin, H. (1995) *Biochemistry 34*, 9059−9070.

Southern, E. M. (1975) *J. Mol. Biol. 98*, 503−517.

Stiefel, E. I., & George, G. N. (1994) in *Ferredoxins, Hydrogenases and Nitrogenases; Metal-Sulfide Proteins in Bioinorganic Chemistry* (Bertini, I., Ed.) pp 365−455, University Science Book.

Takahashi, Y., Goldschmidt-Clermont, M., Soen, S.-Y., Franzen, L.-G., & Rochaix, J.-D. (1991) *EMBO J. 10*, 2033−2040.

Takahashi, Y., Goldschmidt-Clermont, M., & Rochaix, J.-D. (1992) in *Research in Photosynthesis* (Murata, N. E., Ed.) Vol. III, pp 393−396, Kluwer Academic Publishers, Dordrecht, The Netherlands.

Yu, J., Smart, L. B., Jung, Y.-S., Golbeck, J. H., & McIntosh, L. (1996) *Plant Mol. Biol. 29*, 331−342.

Yu, L., Bryant, D. A., & Golbeck, J. H. (1995) *Biochemistry 34*, 7861−7868.

Zhao, J., Li, N., Warren, P. V., Golbeck, J. H., & Bryant, D. A. (1992) *Biochemistry 31*, 5093−5099.

BI962244V